Mechanistic Studies of Ligand Fluxionality in $[M(\eta^5\text{-Cp})(\eta^1\text{-Cp})(L)_2]^n$

Alireza Ariafard,*,†,‡ Elham S. Tabatabaie,† and Brian F. Yates*,‡

Department of Chemistry, Faculty of Science, Central Tehran Branch, Islamic Azad University, Shahrak Gharb, Tehran, Iran, and School of Chemistry, University of Tasmania, Private Bag 75, Hobart TAS 7001, Australia

Received: November 14, 2008; Revised Manuscript Received: January 14, 2009

Density functional theory has been used to provide a thorough investigation of the mechanistic factors affecting Cp ligand fluxionality in a series of organometallic complexes, $[M(\eta^5\text{-Cp})(\eta^1\text{-Cp})(L)_2]^n$, involving different metals, different oxidation states, and different ligands. Excellent agreement with experiment for the barrier heights for the 1,5-shift were obtained for the complexes $[Fe(\eta^5\text{-Cp}^*)(\eta^1\text{-Cp})(CO)_2]$ and $[Fe(\eta^5\text{-Cp})(\eta^1\text{-Cp})(CO)_2]$. For the range of complexes studied, the barriers have been successfully rationalized in terms of hyperconjugation, metal−Cp bond strength, and steric effects. In addition, the $\eta^1-\eta^5$ interconversion of the Cp binding mode is shown to be a high-energy process, consistent with experimental observations. The L substitution reactions by η^1-Cp are quite sensitive to the nature of the metal center and ancillary ligand. A detailed theoretical explanation of the factors involved in all of these transformations is provided.

Introduction

In 1966, Cotton and co-workers demonstrated for the first time that metal migration around η^1-Cp in $[Fe(\eta^5\text{-Cp})(\eta^1\text{-Cp})(CO)_2]$ can occur via sequential 1,5-shifts.[1] Later on, numerous studies were made in order to electronically investigate the 1,5-shift process in a variety of the η^1-Cp transition metal systems.[2−10] A similar migration of main group elements in η^1-Cp compounds was also observed. The rate for the migration in the η^1-Cp compounds increases as the size of the central atom increases. This was rationalized in terms of the fact that the E−C(η^1-Cp) bond, where E = main group elements, is more readily cleaved as E becomes heavier.[11] On the other hand, both experimentally[11−14] and theoretically,[15] it was corroborated that there exists an excellent correlation between the rate of 1,5-shift and the degree of $\sigma-\pi$ hyperconjugation (delocalization of the E−C(η^1-Cp) σ bond to adjacent π^* orbitals on η^1-Cp).

The interconversion between η^1- and η^5-Cp bonding modes in transition metal complexes $[M(\eta^5\text{-Cp})(\eta^1\text{-Cp})L_m]^n$ has also been the subject of several previous theoretical[16,17] and experimental[6,10,18−21] studies. A kinetically difficult process was found for the η^1/η^5 interconversion of the cyclopentadienyl ligands in $[Fe(\eta^5\text{-Cp})(\eta^1\text{-Cp})(CO)_2]$.[5] In contrast, NMR data, supported by theoretical studies, predicted a rapid interconversion between the η^1- and η^5-Cp bonding modes in $[Ti(\eta^5\text{-Cp})_2(\eta^1\text{-Cp})Cl]$,[6,18] $[Mo(\eta^5\text{-Cp})(\eta^1\text{-Cp})(N^tBu)_2]$,[19] and $[Nb(\eta^5\text{-Cp})_2(\eta^1\text{-Cp})(N^tBu)]$.[20] These results demonstrated that the rate of the rearrangement process depends strongly on the nature of the metal center and the ancillary ligands.

It was also established that warming $[Fe(\eta^5\text{-Cp})(\eta^1\text{-Cp})(CO)_2]$ leads to dissociation of carbonyl ligands and formation of the sandwich complex $[Fe(\eta^5\text{-Cp})_2]$.[5,22] Irradiation of $[Fe(\eta^5\text{-Cp})(\eta^1\text{-Cp})(CO)_2]$ at low temperature gives $[Fe(\eta^5\text{-Cp})(\eta^3\text{-Cp})(CO)] + CO$. The monocarbonyl intermediate $[Fe(\eta^5\text{-Cp})(\eta^3\text{-Cp})(CO)]$ is sensitive to thermal conditions, meaning that the first CO dissociation from $[Fe(\eta^5\text{-Cp})(\eta^1\text{-Cp})(CO)_2]$ is more difficult than the second one.[23]

In this paper, we wish to systematically study the $\sigma-\pi$ hyperconjugation, the 1,5-metal shift, the η^5-Cp/η^1-Cp interconversion, and the CO substitution by η^1-Cp in the complexes $[M(\eta^5\text{-Cp})(\eta^1\text{-Cp})(CO)_2]^n$ (M = Mn, $n = -1$; M = Fe, Ru, Os, $n = 0$; M = Co, $n = +1$), $[Fe(\eta^5\text{-Cp})(\eta^1\text{-Cp})(PMe_3)_2]$, and $[Fe(\eta^5\text{-Cp}^*)(\eta^1\text{-Cp})(CO)_2]$ ($Cp^* = C_5Me_5$) using density functional theory (DFT). The choice of the model complexes was made with the goal to investigate the effect of charge, metal center, ancillary ligand, and the Me substituents on η^5-Cp on the fluxional behaviors and the CO dissociation mechanism. This study provides a good opportunity to investigate whether or not the degree of the $\sigma-\pi$ hyperconjugation affects the rate of the fluxional behaviors in transition metal complexes $[M(\eta^5\text{-Cp})(\eta^1\text{-Cp})L_m]^n$.

Computational Details

Gaussian 03[24] was used to fully optimize all the structures reported in this paper at the B3LYP level[25−27] of density functional theory. The effective core potentials of Hay and Wadt with double-ζ valence basis sets (LanL2DZ)[28−30] were chosen to describe Fe, Ru, Os, Mn, Co, and P. The 6-31G(d) basis set was used for other atoms.[31] Polarization functions were also added for Fe ($\zeta_f = 2.462$), Ru ($\zeta_f = 1.235$), Os ($\zeta_f = 0.886$), Mn ($\zeta_f = 2.195$), Co ($\zeta_f = 1.941$)[32] and P ($\zeta_d = 0.387$).[33] This basis set combination will be referred to as BS1. Frequency calculations were carried out at the same level of theory for structural optimization. To further refine the energies obtained from the B3LYP/BS1 calculations, we carried out single-point energy calculations for all the structures with a larger basis set (BS2). BS2 comprises the SDDALL[34,35] basis set with associated ECPs for the transition metals and 6-311++G(2d,p) basis set for the other atoms. To estimate the corresponding Gibbs free energies, the entropy corrections were calculated at the B3LYP/BS1 level and added to the B3LYP/BS2 total energies. We have used the B3LYP/BS2//B3LYP/BS1 energies throughout the paper unless otherwise stated. The natural bond orbital (NBO)

* Corresponding author. E-mail: ariafard@yahoo.com.
† Islamic Azad University.
‡ University of Tasmania.

10.1021/jp810032a CCC: $40.75
Published on Web 03/04/2009

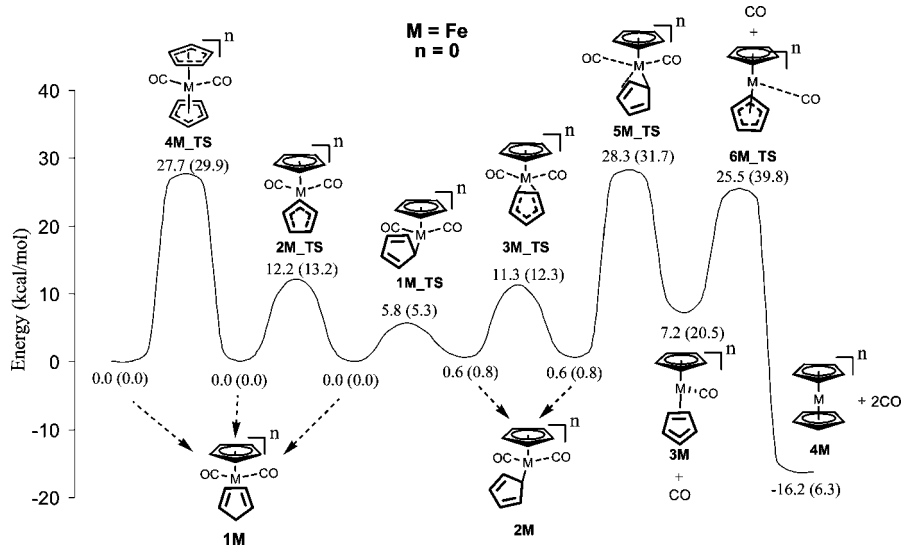

Figure 1. Energy profile calculated for the rotation of η^1-Cp, 1,5-shift, η^5-Cp/η^1-Cp interconversion, and first and second CO substitution reactions in $[M(\eta^5\text{-Cp*})(\eta^1\text{-Cp})(CO)_2]^n$, where M = Fe and $n = 0$. The relative free energies and potential energies (in parentheses) obtained from the B3LYP/BS2//B3LYP/BS1 calculations are given in kcal/mol.

TABLE 1: Energy Changes in the Rotation of η^1-Cp, 1,5-Shift, η^5-Cp/η^1-Cp Interconversion, and First and Second CO Substitution Reactions in $[M(\eta^5\text{-Cp*})(\eta^1\text{-Cp})(CO)_2]^n$, Where M = Mn, $n = -1$; M = Fe, Ru, Os, $n = 0$; M = Co, $n = +1$[a]

M	1M	2M	3M	4M	1M_TS	2M_TS	3M_TS	4M_TS	5M_TS	6M_TS
Co	0.0	−0.4	−5.5	−40.5	5.5	12.5	10.7	28.9	21.8	5.6
	(0.0)	(−0.3)	(6.6)	(−17.5)	(5.4)	(13.7)	(11.8)	(30.8)	(18.8)	(19.5)
Fe	0.0	0.6	9.9	−16.2	5.8	12.2	11.3	27.7	28.3	25.5
	(0.0)	(0.8)	(23.2)	(6.3)	(5.3)	(13.2)	(12.3)	(29.9)	(31.7)	(39.8)
Mn	0.0	2.6	27.8	25.4	5.7	5.8	8.3	20.1	36.9	53.6
	(0.0)	(2.3)	(38.8)	(49.3)	(4.9)	(5.8)	(8.2)	(21.4)	(39.6)	(66.9)
Ru	0.0	1.6	21.3	−0.7	5.6	14.6	14.9	26.4	36.5	40.1
	(0.0)	(1.6)	(31.5)	(21.0)	(4.4)	(15.2)	(15.8)	(27.8)	(39.2)	(52.9)
Os	0.0	2.0	22.8	11.5	5.8	14.9	18.1	28.4	43.2	52.1
	(0.0)	(1.9)	(35.2)	(33.9)	(4.6)	(16.8)	(18.6)	(29.7)	(46.5)	(65.3)

[a] The structure labels are shown in Figure 1. The relative free energies and potential energies (in parentheses) obtained from the B3LYP/BS2//B3LYP/BS1 calculations are given in kcal/mol.

program,[36] as implemented in Gaussian 03, was used to obtain natural populations of atoms.

Results and Discussion

Figure 1 shows the energy profile for the CO dissociation process and the fluxional behaviors in $[Fe(\eta^5\text{-Cp})(\eta^1\text{-Cp})(CO)_2]$. The results of similar calculations for the other complexes $[M(\eta^5\text{-Cp})(\eta^1\text{-Cp})(CO)_2]^n$ are listed in Table 1. The optimized geometries with selected structural parameters for some of the species given in Figure 1 are shown in Figure 2. The detailed structures of other calculated complexes, $[M(\eta^5\text{-Cp})(\eta^1\text{-Cp})(CO)_2]^n$, where M = Mn, Ru, Os, and Co, can be found in the Supporting Information.

Consistent with the previously undertaken studies by Romao and Veiros on $[Mo(\eta^5\text{-Cp})(\eta^1\text{-Cp})(N^tBu)_2]$,[17] $[M(\eta^5\text{-Cp})(\eta^1\text{-Cp})(CO)_2]^n$ can exist in the two isomers **1M** and **2M** due to the relative orientations of the η^1-Cp ligands. In isomer **1M**, the η^1-Cp ligand points toward the η^5-Cp ligand, while in isomer **2M** the η^1-Cp ligand points toward one of the CO ligands. **1Fe** is calculated to be about 0.6 kcal/mol more stable than **2Fe**.[37] This result is in good agreement with the experimental observation in which **1Fe** is the only structure reported for $[Fe(\eta^5\text{-Cp})(\eta^1\text{-Cp})(CO)_2]$. **1M_TS** is the transition state structure connecting **1M** to **2M**. The free energy barriers of the **1M**→**2M** transformations for all the complexes calculated are comparable, indicating that the rotational barrier of η^1-Cp around the M−C σ bond is independent of the identity of the metal center.

***σ*−*π* Hyperconjugation.** To estimate the stabilization energy resulting from the delocalization of the M−C(η^1-C_5H_5) σ bond in the η^1-Cp ring, we designed the isodesmic reaction shown in Figure 3.[38] In this isodesmic reaction, the η^1-Cp ring is broken in such a way that the resulting small species does not contain conjugation. The M−C(η^1-C_5H_5) hyperconjugation in complexes **1M** can be described by a resonance hybrid of the five Lewis structures shown in Scheme 1. A greater degree of resonance in the η^1-Cp ring gives rise to a higher stability of **1M**. The largest ΔE reaction energy is found for **1Mn**, while the smallest value for **1Co** (Figure 3). Our calculations show a large dependence of hyperconjugation on the charge of the system and a smaller dependence on the metal center row. From Figure 3, we can also see that the hyperconjugation energy decreases down a group. A net negative charge on the complex raises the hyperconjugation energy, and a net positive charge lowers it. This indicates that a decrease in charge facilitates the M−C(η^1-C_5H_5) σ bond delocalization in the η^1-Cp ring. The decreased net charge on the 18-electron complexes, leading to a low oxidation state for the metal center, gives rise to a decrease in the electronegativity of M. In such a case, the M−C(η^1-C_5H_5) σ bond is considerably polarized toward C, the bond becomes significantly ionic in character, and consequently the hyperconjugation is promoted. To support the claim, the NBO analysis

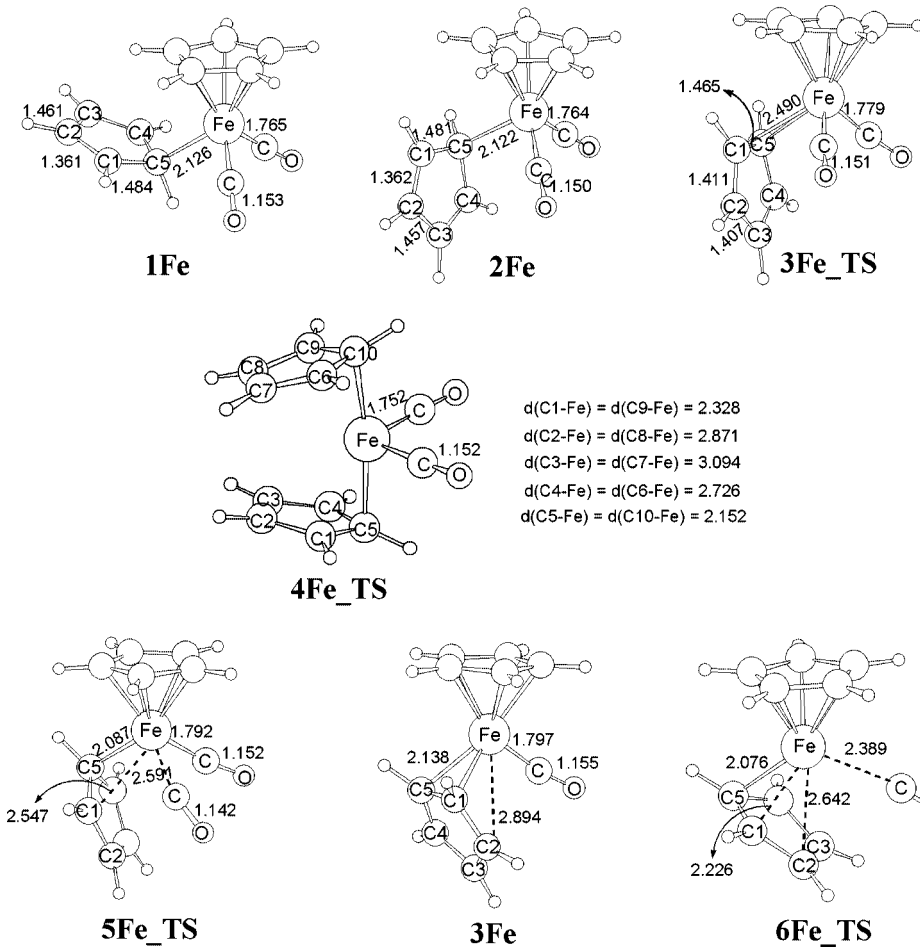

Figure 2. Optimized structures with selected structural parameters (bond length in Å) for some of the species involved in the energy profile shown in Figure 1.

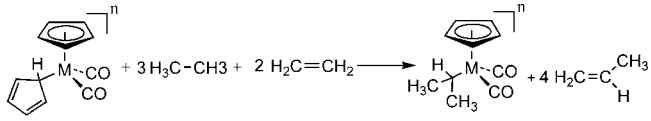

M	n	ΔE (kcal/mol)
Mn	-1	19.0
Fe	0	7.1
Ru	0	5.6
Os	0	5.1
Co	+1	0.5

Figure 3. Reaction energies obtained from the isodesmic equation using the B3LYP/BS2//B3LYP/BS1 calculations.

was carried out using the B3LYP/BS2//B3LYP/BS1 calculations. On the basis of the analysis, the C% contribution to the M−C(η^1-C_5H_5) bond was calculated to be 69.7, 55.9, 50.3% for **1Mn**, **1Fe**, and **1Co**, respectively. The NBO partial charge on the bound η^1-Cp moiety is −0.493, −0.208, and 0.063 for **1Mn**, **1Fe**, and **1Co**, respectively. It follows from these results that decreasing the charge on the complexes indeed increases the contribution of the Lewis structures **II**−**V** (Scheme 1) to **1M**, enhancing the hyperconjugation energy. The lower electronegativity of the first row transition metal versus the second or third row is also the main reason why the hyperconjugation energy decreases on going down a group. The slightly smaller hyperconjugation energy for **1Os** compared to **1Ru** can probably be attributed to the different strength of the metal−carbon σ bonds in the isodesmic reaction.

Support of the argument above can also be found from nucleus-independent chemical shift (NICS)[39] calculations (a measure of aromaticity) (Table 2). NICS values at $z = 0$ were calculated at the center of the η^1-Cp ring in the complexes, found by averaging the coordinates of the five carbon atoms forming the ring. NICS values at $z = 1$ were calculated at a point 1.0 Å away from the center of the η^1-Cp ring on the opposite side of the metal, in a direction perpendicular to the plane of the ring. Both sets of results (Table 2) show that the most negative NICS values are calculated for **1Mn**, highlighting that the contribution of the Lewis structures **II**−**V** to the real structure is significant while the least negative value for **1Co** suggests that the contribution of the Lewis structures **II**−**V** is negligible.

1,5-Shift Mechanism. Experimentally and theoretically, it has been established that metal migration around the η^1-Cp ring occurs through a 1,5-shift mechanism.[8,17] Table 1 lists the energy barriers calculated for the 1,5-metal shift for all the complexes.[40] As illustrated in Figure 1, there are two possible pathways for the 1,5-metal shift. One occurs through transition state **2M_TS** (a transition state connecting two equivalent **1M** species), and the other passes through transition state **3M_TS**, which connects two equivalent **2M** species. In the case of M = Fe, the lowest energy pathway corresponds to the sequence **1Fe** → **1Fe_TS** → **2Fe** → **3Fe_TS** → **2Fe** → **1Fe_TS** → **1Fe**. The calculated energy barrier for [Fe(η^5-Cp)(η^1-Cp)$(CO)_2$] (11.3 kcal/mol) is in excellent agreement with the experimental value of 11.1 ± 0.2 kcal/mol.[41] The computational results suggest that the η^1-Cp complexes can undergo the 1,5-shift via an I (interchange) mechanism in that the M−C5 bond is mainly broken while the

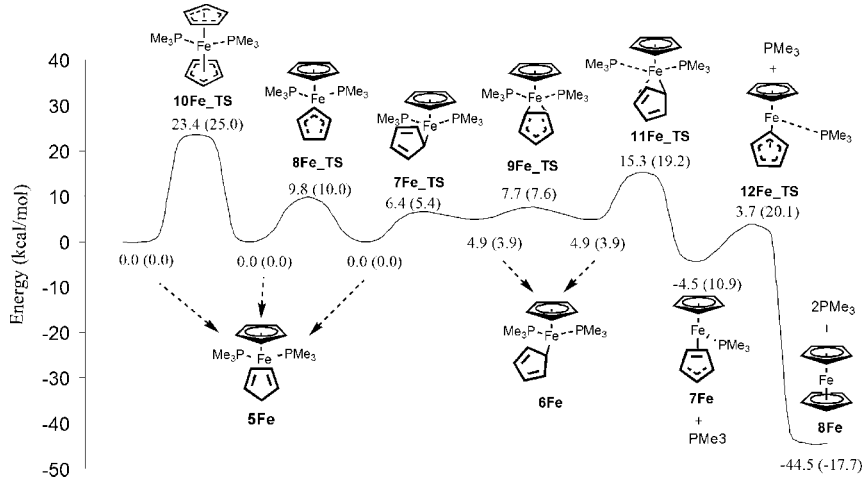

Figure 4. Energy profile calculated for the rotation of η^1-Cp, 1,5-shift, η^5-Cp/η^1-Cp interconversion, and first and second PMe_3 substitution reactions in $[Fe(\eta^5\text{-Cp})(\eta^1\text{-Cp})(PMe_3)_2]$. The relative free energies and potential energies (in parentheses) obtained from the B3LYP/BS2//B3LYP/BS1 calculations are given in kcal/mol.

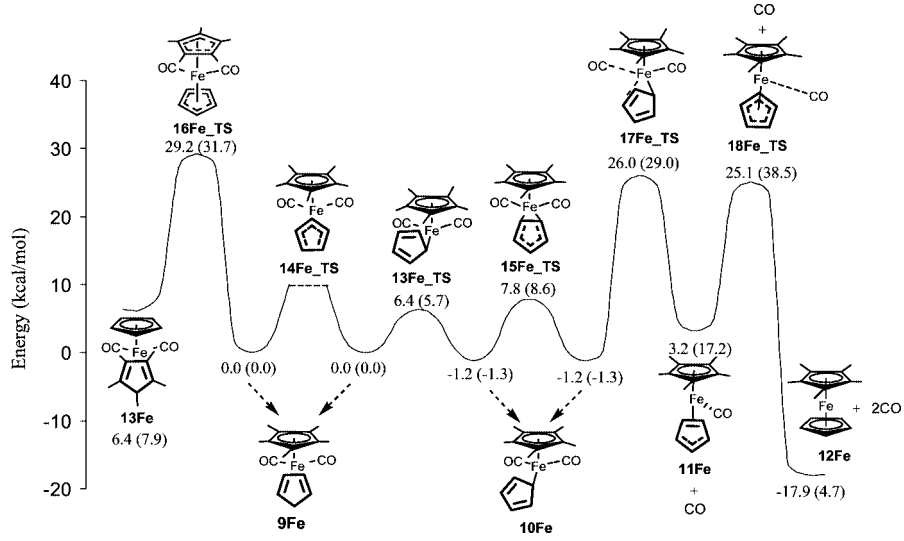

Figure 5. Energy profile calculated for the rotation of η^1-Cp, 1,5-shift, η^5-Cp/η^1-Cp interconversion, and first and second CO substitution reactions in $[Fe(\eta^5\text{-Cp*})(\eta^1\text{-Cp})(CO)_2]$. The relative free energies and potential energies (in parentheses) obtained from the B3LYP/BS2//B3LYP/BS1 calculations are given in kcal/mol. **14Fe_TS** could not be located.

SCHEME 1

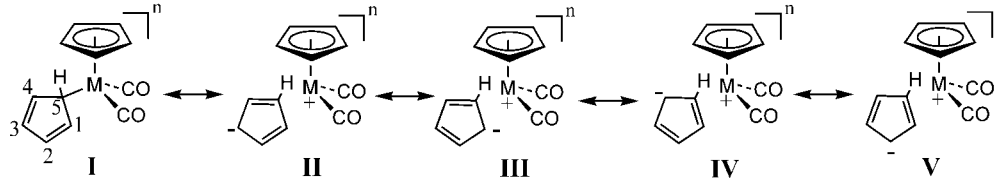

TABLE 2: NICS(0) and NICS(1) Values Calculated for the Species 1M Using the B3LYP/BS2//B3LYP/BS1 Calculations

		1Co	1Fe	1Mn	1Ru	1Os
NICS	$z = 0$	0.3	−6.1	−11.1	−4.6	−4.5
	$z = 1$	−1.9	−6.0	−8.6	−5.2	−5.3

new M−C1 bond is partially formed. For instance, the Fe−C5 distance lengthens from 2.126 Å in **1Fe** to 2.490 Å in **3Fe_TS** and the Fe−C1 distance shortens from 3.00 Å in **1Fe** to 2.490 Å in **3Fe_TS** (Figure 2). A similar trend was also obtained for their corresponding bond indices; the bond order of Fe−C5 and Fe−C1 is calculated to be 0.485 and 0.019 for **1Fe**, and 0.206 and 0.206 for **3Fe_TS**, respectively. In view of the fact that the **1M** (or **2M**) complexes conform to the 18-electron rule, while the **2M_TS** (or **3M_TS**) transition structures may be thought of as 16-electron complexes, the above results agree with the experimental evidence that organometallic reactions occur by 18 ↔ 16 electron sequences.

As expected, the increased M−C(η^1-Cp) hyperconjugation causes an increase in the contribution of the Lewis structure **III** to the η^1-Cp complexes (Scheme 1). With greater participation of **III**, the C1 nucleophilicity for attacking the metal center increases. This electronic feature is capable of facilitating the achievement of the transition states for the 1,5-shift process. As a result, both the nucleophilic attack of C1 and the breaking of the M−C5 bond take place simultaneously and lead to the formation of transition states **2M_TS** and **3M_TS.** The resonance forms **VII** and **IX** (Scheme 2) are the predominate

SCHEME 2

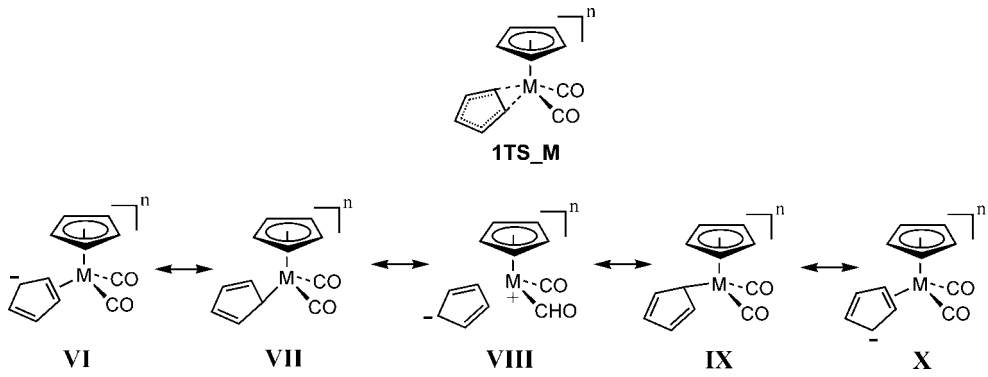

TABLE 3: Bond Distances (Å) in Transition Structures 2M_TS

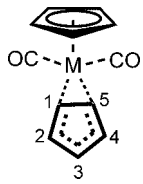

M	C1−C5	C1−C2	C2−C3	C3−C4	C5−C1
Co	1.503	1.391	1.416	1.416	1.391
Fe	1.465	1.410	1.407	1.407	1.410
Mn	1.443	1.416	1.408	1.408	1.416
Ru	1.474	1.407	1.408	1.408	1.407
Os	1.475	1.409	1.407	1.407	1.409

contributors to the bonding of the transition states. Examination of the calculated structural parameters shown in Table 3 supports the claim and shows that the resonance forms **VII** and **IX** contribute to the real transition structures with a comparable involvement. The C1−C2, C2−C3, C3−C4, C4−C5 bond distances in all the transition structures are approximately equal, while the C1−C5 bond distance is significantly longer than the other C−C bonds (Table 3).

From Table 1, one can see that the energy barrier of the 1,5-shift for **1Mn** (**2Mn_TS**) is lower than the others. The metal migration for **1Fe** is easier than for the heavier homologous **1Ru** and **1Os**. The results also indicate that the 1,5-migration barrier for **1Co** is slightly lower than that for **1Ru**. From these results, one cannot observe any good correlation between the calculated hyperconjugation energies (Figure 3) and the 1,5-shift barriers (Table 1). Therefore, it is expected that, in addition to the hyperconjugation energy, the M−C(η^1-Cp) bond strength also plays a role in determining the barriers. Using the basis set BS2, the M−C(η^1-Cp) bond energies were estimated to be 19.1 kcal/mol for **1Fe**, 34.1 kcal/mol for **1Ru**, 37.7 kcal/mol for **1Os**, and 15.2 kcal/mol for **1Co** using the B3LYP/BS2//B3LYP/BS1 calculations. Since the hyperconjugation energies calculated for **1Os**, **1Ru**, and **1Co** are small (Figure 3), the higher 1,5-shift barrier of **1Os** and **1Ru** over **1Co** can be attributed to the stronger Os−C(η^1-Cp) and Ru−C(η^1-Cp) bonds. In contrast, for **1Mn**, the net negative charge on the complex and the low formal oxidation state of 1 for the metal center enhances the hyperconjugation energy. The strong hyperconjugation in **1Mn** is the reason for the lower 1,5-shift barrier, although the bond energy calculated for Mn−C(η^1-Cp) (37.7 kcal/mol) is significantly high. It follows from these results that, for the anionic complex **1Mn**, the Mn−C(η^1-Cp) hyperconjugation is the dominant factor contributing to the ease of the 1,5-shift process. In contrast, for the cationic and neutral complexes, the M−C($\eta^1C_5H_5$) bond strength plays a more dominant role in metal migration.

SCHEME 3

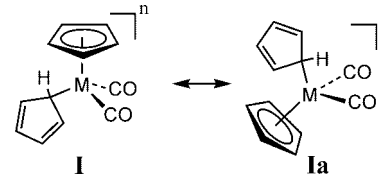

At this point, it is noteworthy to compare our 1,5-shift results with those for the η^1-Cp compounds of main-group elements. Contrary to the trend we found for the η^1-Cp transition metal complexes, the heavier elements in a given main group exhibit lower 1,5-shift barriers.[11] This difference can be attributed to the fact that the hyperconjugation energy increases as we move down a main group.[42] In addition, the M−C(η^1-Cp) bond strength also decreases in the same direction.[11]

***η*^{5}-Cp/*η*^{1}-Cp Interconversion.** The mechanism of the interconversion between the η^5-Cp and η^1-Cp ligands is another interesting point to be addressed. The η^5-Cp/η^1-Cp interconversion proceeds via a one-step mechanism in which **4M_TS** is midway between the two products shown in Scheme 3. In **4M_TS**, the two exchanging Cp ligands adopt a pseudo-η^3 coordination mode and are structurally related to each other by a C_2 symmetry axis. Figure 2 shows the calculated geometry of **3Fe_TS**, while the detailed structure of other transition states is given in the Supporting Information.

In comparison with 1,5-metal migration, this process has a very much higher barrier. Our calculations showed that, for M = Fe, the barrier to CO dissociation and to η^5-Cp/η^1-Cp interconversion is comparable (Figure 1). This result is consistent with the experimental observation that no η^5-Cp/η^1-Cp interconversion for [Fe(η^5-Cp)(η^1-Cp)(CO)$_2$] was reported and all attempts led to decomposition of the complex.[5] The barriers for **1M** → **4M_TS** → **1M** (Table 1) increase in the order M = Mn < Ru < Fe < Os < Co, indicating that the η^5-Cp/η^1-Cp interconversion barrier is lowest for the anionic complexes and highest for the cationic complexes, with the neutral complexes in between. A plausible explanation for these findings is as follows. The η^5-Cp ligand in [M(η^5-Cp)(η^1-Cp)(CO)$_2$]^n is bound to the metal center as a L_2X ligand[43] in which X stands for a ligand acting as a 1e donor and forms a M−X covalent bond, whereas L refers to a ligand acting as a lone-pair donor and forms a M−L coordinate bond. Upon going from **1M** to **4M_TS**, the hapticity of the Cp ligand mainly changes from η^5-L_2X to η^1-X (see **4Fe_TS** in Figure 2), suggesting that dissociation of the two M−L bonds should be the most important factor in controlling the rate of interconversion. An earlier calculation established that the donation of the electron

TABLE 4: Calculated NBO Partial Charges on η^5-Cp ($q_{(\eta^5\text{-Cp})}$) and η^1-Cp ($q_{(\eta^1\text{-Cp})}$) of 1M[a]

	1Co	1Fe	1Mn	1Ru	1Os
$q_{(\eta^5\text{-Cp})}$	+0.597	+0.277	−0.027	+0.194	−0.085
$q_{(\eta^1\text{-Cp})}$	+0.063	−0.208	−0.493	−0.173	−0.292
Δq	+0.534	+0.485	+0.466	+0.368	+0.206

[a] Δq refers to the difference between these two partial charge.

density on η^5-Cp to the metal center, π donation, is the dominating bonding interaction.[44] A comparison of the NBO partial charges of η^5-Cp with η^1-Cp in a given complex **1M** shows some support for the argument above. The difference in the NBO charges between η^5-Cp (η^5-L_2X) and η^1-Cp (η^1-X) (Δq in Table 4) is always positive, suggesting that the largest contribution of the η^4-L_2 moiety of η^5-Cp to the bonding interaction comes from the η^4-$L_2 \rightarrow$ metal π-donation. Therefore, we expect the strongest M−L bonds in the cationic complexes and the weakest M−L bonds in the anionic complexes. The stronger the M−L bonds, the higher the interconversion barrier. In addition, the Os metal center, which possesses more diffuse d orbitals when compared to M = Ru, more strongly interacts with η^5-Cp, making the η^5-Cp/η^1-Cp rearrangement more difficult than for M = Ru.

It is of interest to note that the calculated interconversion barrier for the complexes $[M(\eta^5\text{-Cp})(\eta^1\text{-Cp})(CO)_2]^n$ are much higher than for $[Mo(\eta^5\text{-Cp})(\eta^1\text{-Cp})(N^tBu)_2]$ (15 kcal/mol).[17] In the transition state of $[Mo(\eta^5\text{-Cp})(\eta^1\text{-Cp})(N^tBu)_2]$, the N-lone pairs interact with the available d_π orbitals of Mo, lowering the interconversion barrier. This electronic effect, leading to the stabilization of the transition state, is absent in the systems studied here.

Decarbonylation Reaction. It was observed experimentally that the loss of CO can occur upon warming of such η^1-Cp complexes, yielding the conversions of η^1-Cp to η^3-Cp and subsequently to η^5-Cp.[5,22,23] To predict how different metals with different oxidation states in $[M(\eta^5\text{-Cp})(\eta^1\text{-Cp})(CO)_2]^n$ affect the substitution reaction rates, we calculated the potential energy surface for the first and second CO substitution by η^1-Cp (see Table 1 and Figure 1). As mentioned above, an η^3-Cp complex was proposed to be an intermediate between the η^1-Cp and η^5-Cp complexes.[23] In contrast, our calculations show that the first CO substitution reaction by η^1-Cp yields an η^2-Cp intermediate instead of an η^3-Cp intermediate as the reaction product. The η^3-Cp complexes are calculated to be first-order saddle points on the PES, connecting two η^2-Cp complexes **3M** to each other. We also found that η^1-Cp-assisted CO substitution, giving **3M**, has a higher barrier than η^2-Cp-assisted CO substitution, giving **4M** (Figure 1 and Table 1). For instance, the barrier from **2Fe** to **3Fe** (27.7 kcal/mol) is calculated to be 9.4 kcal/mol higher than that from **3Fe** to **4Fe** (18.3 kcal/mol). This result, which agrees well with the experimental observations concerning the temperature dependence of CO loss, demonstrates that, in general, **2M** is much less labile than **3M**. Because the substitution reactions proceed via an I_d (dissociative interchange) mechanism, it is expected that the CO ligand should bind more tightly to the metal center in **2M** than in **3M**. We also believe that, in **6M_TS** and **4M**, the aromaticity of the Cp ligand involved in the substitution reaction is noticeably recovered, making the CO substitution easier. This claim finds support from NICS calculations. For example, the NICS(1) values of −5.8, −7.4, −5.1, −11.1, and −17.3 were computed for **2Fe**, **5Fe_TS**, **3Fe**, **6Fe_TS**, and **4Fe**, respectively, suggesting that the relevant Cp ligands benefit from the increased degree of aromaticity in **6Fe_TS** and **4Fe**.

The calculated activation barriers (Table 1) for the substitution reaction are 36.9, 28.3, and 21.8 kcal/mol for **1Mn**, **1Fe**, and **1Co**, respectively, indicating that a decrease in charge impedes the CO substitution reaction. The trend reflects the back-bonding power of the metal centers, which increases in strength by decreasing the net charge on the complex. Since CO acts as a π-acceptor ligand, the M−CO interaction becomes stronger as the electron donor ability of M increases. The stronger the M−CO bond, the higher the activation barrier of the CO substitution reaction. Our calculations also show that the corresponding reaction barriers for the group 8 triad increase as one goes from **1Fe** (28.3 kcal/mol) to **1Ru** (36.5 kcal/mol) and then to **1Os** (43.2 kcal/mol), suggesting that the M−CO bond in **1Os** is stronger than in **1Fe** and **1Ru**. The overall reaction from **1M** to **4M** is endothermic for M = Mn and Os while it is exothermic for M = Co and Fe. This reaction is nearly thermoneutral for M = Ru, with a reaction energy of −0.7 kcal/mol. It follows from these results that the formation of **4M** from **1M** for anionic complexes as well as heavier transition metal complexes is unlikely. Conversely, a decrease of the electron density on the metal center of $[M(\eta^5\text{-Cp})(\eta^1\text{-Cp})(CO)_2]^n$ leads to a dramatic enhancement in reactivity of the complex toward the CO dissociation reaction.

Effect of the Ancillary Ligand. We have also investigated the effect of the ancillary ligand on the barrier of the 1,5-shift, η^5-Cp/η^1-Cp interconversion, and L substitution reaction using the model complex $[Fe(\eta^5\text{-Cp})(\eta^1\text{-Cp})(PMe_3)_2]$. The results of the calculations show that the barriers for 1,5-shift (7.7 kcal/mol) and the interconversion (23.4 kcal/mol) of the PMe_3 system are lower than that of the corresponding CO system (see Figures 1 and 4). Indeed, PMe_3 is a stronger σ-donor and a poorer π-acceptor than CO. This electronic feature increases the electron density on Fe, which leads to a decreased electronegativity of Fe. This, in turn, enhances the Fe−C(η^1-Cp) hyperconjugation as evidenced by calculating the hyperconjugation energy; **5Fe** (13.9 kcal/mol) has larger hyperconjugation energy than **1Fe** (7.1 kcal/mol). The charge carried by the η^1-Cp ligand in **5Fe** (−0.438) is more negative than in **1Fe** (−0.208). Thus, in view of the stronger Fe−C(η^1-Cp) bond in **5Fe** (25.5 kcal/mol) than in **1Fe** (19.1 kcal/mol), the lower 1,5-shift barrier calculated for **5Fe** can be explained in terms of hyperconjugation. With increasing electron density on Fe as the more basic PMe_3 ligand is employed, the interaction between Fe and the η^4-L_2 moiety of η^5-Cp weakens, and consequently, the η^5-Cp/η^1-Cp interconversion is facilitated.

The η^1-Cp- and η^2-Cp-assisted PMe_3 substitution reactions have larger reaction energies and require lower activation barriers when compared to the η^1-Cp- and η^2-Cp-assisted CO substitution reactions. This result indicates the much better reactivity of **5Fe** vs **1Fe** toward ligand dissociation. Thus, it appears that the presence of (π) electron-withdrawing groups such as CO on Fe is necessary to maximize the stability of such η^1-Cp complexes. These results also explain why, experimentally, the formation of such η^1-Cp iron complexes with phosphine ligands requires highly strained ferrocenophanes as reactants (for example, see **1**).[45,46] Indeed, it is expected that, due to high strain energy, highly strained ferrocenophanes are less stable than ferrocene, energetically favoring the formation of η^1-Cp complexes. Studies are now in progress to further understand how the ring strains facilitate the formation of η^1-Cp complexes from the reaction of metallophanes with phosphines.

Effect of Methyl Substituents on the η^5-Cp Ring. To elucidate the role of the methyl substituents on the η^5-Cp ring

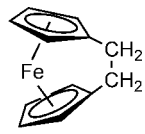

1

in the reactivity of the η^1-Cp complexes toward fluxionality and ligand dissociation, we extended the investigations to [Fe(η^5-Cp*)(η^1-Cp)(CO)$_2$] (Cp* = C_5Me_5) (Figure 5). Our calculations show that, in accord with the experimental findings,[41] **9Fe** is less stable than **10Fe**, most likely due to steric reasons. The replacement of the H atoms of the η^5-Cp ring in [Fe(η^5-Cp)(η^1-Cp)(CO)$_2$] with electron-donating Me groups provides only a small enhancement in the hyperconjugation energy (7.9 kcal/mol for **9Fe** vs 7.1 kcal/mol for **1Fe**). The calculated activation energy for 1,5-metal shift through **10Fe → 15Fe_TS → 10Fe** (9.0 kcal/mol) is in excellent agreement with the experimental value (9.6 ± 0.2). All attempts to locate the transition state **14Fe_TS** were unsuccessful. A combination of two important factors, steric effects and hyperconjugation, explain the reduction in the 1,5-shift barrier of [Fe(η^5-Cp*)(η^1-Cp)(CO)$_2$] compared with [Fe(η^5-Cp)(η^1-Cp)(CO)$_2$]. In addition, **10Fe** undergoes η^5-Cp*/η^1-Cp interconversion through transition state **16Fe_TS** to form **13Fe**. This interconversion has a higher activation barrier (30.4 kcal/mol) than the **1Fe → 4Fe_TS → 1Fe** interconversion and is endothermic (7.6 kcal/mol). This feature can be rationalized in terms of that fact that, due to presence of the electron-donating Me groups on Cp*, the η^4-L$_2$ moiety of η^5-Cp* in **10Fe** binds to Fe more strongly than the η^4-L$_2$ moiety of η^5-Cp in **13Fe**. A comparison of Figures 1 and 5 also shows that the replacement of Cp with Cp* has little influence on the energy required for the CO dissociation (27.2 kcal/mol for **10Fe → 17Fe_TS → 11Fe** vs 28.3 kcal/mol for **1Fe → 5Fe_TS → 3Fe**).

Conclusion

Density functional theory calculations have been used to study the fluxionality of Cp ligands and the ligand (CO or PMe_3) dissociation reactions in [M(η^5-Cp)(η^1-Cp)(CO)$_2$]^n (M = Mn, $n = -1$; M = Fe, Ru, Os, $n = 0$; M = Co, $n = +1$), [Fe(η^5-Cp)(η^1-Cp)(PMe_3)$_2$], and [Fe(η^5-Cp*)(η^1-Cp)(CO)$_2$] (Cp* = C_5Me_5). In summary, the following conclusions can be made based on the calculation results:

(1) Two different isomers for the η^1-Cp complexes were located. These two isomers are connected to each other via the rotation of η^1-Cp about the M−C(η^1-Cp) bond. The barrier to the rotation was found to be independent of the identity of metal center and ancillary ligands.

(2) The stabilization energies associated with $\sigma-\pi$ hyperconjugation (delocalization of the E−C(η^1-Cp) σ bond to adjacent π^* orbitals on η^1-Cp) decrease as the net charge on the complexes increases. The introduction of strongly electron-donating ancillary ligands such as PMe_3 makes the metal center electron-rich, enhancing the hyperconjugation energy.

(3) For complexes having sufficiently electron-rich metal centers, such as [Mn(η^5-Cp)(η^1-Cp)(CO)$_2$]$^-$ and [Fe(η^5-Cp)(η^1-Cp)(PMe_3)$_2$], hyperconjugation is the dominant factor contributing to the ease of the 1,5-shift process. In contrast, for complexes not having sufficiently electron-rich metal centers, such as the cationic complex [Co(η^5-Cp)(η^1-Cp)(CO)$_2$]$^+$, the M−C($\eta^1C_5H_5$) bond strength plays a more dominant role in metal migration.

(4) The η^5-Cp/η^1-Cp interconversion is much harder than the 1,5-shift process. The barriers to the η^5-Cp/η^1-Cp interconversion increase in the order M = Mn < Ru < Fe < Os < Co, indicating that the η^5-Cp/η^1-Cp interconversion barrier is lowest for the anionic complexes and highest for the cationic complexes, with the neutral complexes in between. A more basic ancillary ligand, making the metal center more electron-rich, lowers the barrier for the process.

(5) The first CO substitution giving an η^2-Cp complex has a higher barrier than the second CO substitution giving an η^5-Cp complex. This behavior was attributed to the increased degree of aromaticity of Cp in the transition state connecting the η^2-Cp complex to the η^5-Cp complex.

(6) An increase of charge on the metal center facilitates the CO substitution reaction in [M(η^5-Cp)(η^1-Cp)(CO)$_2$]^n.

(7) The preference for the CO substitution reaction is smallest when the transition metal center becomes heavier. Heavier metal centers lead to larger barriers for the CO substitution.

(8) The stability of the iron complexes [Fe(η^5-Cp)(η^1-Cp)L$_2$] is mainly reliant on the electronic nature of L. [Fe(η^5-Cp)(η^1-Cp)L$_2$] with L = PMe_3 has a much higher reactivity toward the formation of [Fe(η^5-Cp)$_2$] when compared with L = CO. Indeed, the presence of electron-withdrawing groups such as CO on the metal center maximizes the stability of the η^1-Cp Fe complexes.

(9) [Fe(η^5-Cp*)(η^1-Cp)(CO)$_2$] is lower in energy than [Fe(η^5-Cp)(η^1-Cp*)(CO)$_2$], due to the presence of the electron-donating Me groups on Cp*, which leads to the η^4-L$_2$ moiety of η^5-Cp* binding to Fe more strongly than the η^4-L$_2$ moiety of η^5-Cp.

(10) A combination of two important factors, steric effects and hyperconjugation, causes a reduction in the 1,5-shift barrier of [Fe(η^5-Cp*)(η^1-Cp)(CO)$_2$] compared with that of [Fe(η^5-Cp)(η^1-Cp)(CO)$_2$].

Acknowledgment. A.A. and E.S.T. appreciate the financial support from Islamic Azad University, Central Tehran Branch, Iran. A.A. and B.F.Y. would like to thank the Australian Research Council (ARC) for project funding. We are also indebted to the Australian Partnership for Advanced Computing (APAC) and the Tasmanian Partnership in Advanced Computing (TPAC) for a generous time grant on their parallel computing facilities.

Supporting Information Available: Complete ref 24 and tables giving Cartesian coordinates, potential energies, and Gibbs free energies for all the calculated structures. This material is available free of charge via the Internet at http://pubs.acs.org.

References and Notes

(1) Bennett, M. J., Jr.; Cotton, F. A.; Davison, A.; Faller, J. W.; Lippard, S. J.; Morehouse, S. W. *J. Am. Chem. Soc.* **1966**, *88*, 4371.

(2) Cotton, F. A.; Musco, A.; Yagupski, G. *J. Am. Chem. Soc.* **1967**, *89*, 6136.

(3) Cotton, F. A.; Legzdins, P. *J. Am. Chem. Soc.* **1968**, *90*, 6232.

(4) Calderon, J. L.; Cotton, F. A.; Legzdins, P. *J. Am. Chem. Soc.* **1969**, *91*, 2528.

(5) Calderon, J. L.; Cotton, F. A.; DeBoer, B. G.; Takats, J. *J. Am. Chem. Soc.* **1970**, *92*, 3801.

(6) Calderon, J. L.; Cotton, F. A.; Takats, J. *J. Am. Chem. Soc.* **1971**, *93*, 3587.

(7) Campbell, A. J.; Fyfe, C. A.; Goel, R. G.; Maslowsky, E., Jr.; Senoff, C. V. *J. Am. Chem. Soc.* **1972**, *94*, 8387.

(8) Cotton, F. A. *Inorg. Chem.* **2002**, *41*, 643.

(9) Gridnev, I. D. *Coord. Chem. Rev.* **2008**, *252*, 1798.

(10) For 1,5-shift and η^5-Cp/η^1-Cp interconversion in beryllium complexes, see: Conejo, M. M.; Fernández, R.; Del Río, D.; Carmona, E.; Monge, A.; Ruiz, C. *Chem. Commun.* **2002**, 2916, and references therein.

(11) Jutzi, P. *Chem. Rev.* **1986**, *86*, 983.

(12) Eradock, S.; Findlay, R. H.; Palmer, M. H. *J. Chem. Soc., Dalton Trans.* **1974**, 1650.

(13) Cradock, S.; Ebsworth, E. A. V.; Moretto, H.; Rankin, D. W. H. *J. Chem. Soc., Dalton Trans.* **1975**, 390.
(14) Ustynyuk, Yu. A.; Zakharov, P. J.; Azizov, A. A.; Potakov, V. K.; Pribytkova, J. M. *J. Organomet. Chem.* **1975**, *88*, 37.
(15) Nori-Shargh, D.; Roohi, F.; Deyhimi, F.; Naeem-Abyaneh, R. *J. Mol. Struct (THEOCHEM)* **2006**, *763*, 21.
(16) Hansen, L. M.; Marynick, D. S. *J. Am. Chem. Soc.* **1988**, *110*, 2358.
(17) Romão, C. C.; Veiros, L. F. *Organometallics* **2007**, *26*, 1777.
(18) Calderon, J. L.; Cotton, F. A.; DeBoer, B. G.; Takats, J. *Ibid.* **1971**, *93*, 3592.
(19) Radius, U.; Sundermeyer, J.; Peters, K.; von Schnering, H.-G. *Eur. J. Inorg. Chem.* **2001**, 1617.
(20) Green, M. L. H.; Michaelidou, D. M.; Mountford, P.; Suárez, A. G.; Wong, L.-L. *J. Chem. Soc., Dalton Trans.* **1993**, 1593.
(21) Fernández, R.; Resa, I.; Del Río, D.; Carmona, E.; Gutiérrez-Puebla, E.; Monge, Á. *Organometallics* **2003**, *22*, 381.
(22) Stradiotto, M.; Hughes, D. W.; Bain, A. D.; Brook, M. A.; McGlinchey, M. J. *Organometallics* **1997**, *16*, 5563.
(23) Beimont, J. A.; Wrighton, M. S. *Organometallics* **1986**, *5*, 1421.
(24) Frisch, M. J.; et al. *Gaussian 03, revision B.05*; Gaussian, Inc.: Pittsburgh, PA, 2003.
(25) Lee, C. T.; Yang, W. T.; Parr, R. G. *Phys. Rev. B* **1988**, *37*, 785.
(26) Becke, A. D. *J. Chem. Phys.* **1993**, *98*, 5648.
(27) Miehlich, B.; Savin, A.; Stoll, H.; Preuss, H. *Chem. Phys. Lett.* **1989**, *157*, 200.
(28) Hay, P. J.; Wadt, W. R. *J. Chem. Phys.* **1985**, *82*, 270.
(29) Wadt, W. R.; Hay, P. J. *J. Chem. Phys.* **1985**, *82*, 284.
(30) Hay, P. J.; Wadt, W. R. *J. Chem. Phys.* **1985**, *82*, 299.
(31) Hariharan, P. C.; Pople, J. A. *Theor. Chim. Acta* **1973**, *28*, 213.
(32) Ehlers, A. W.; Bohme, M.; Dapprich, S.; Gobbi, A.; Hollwarth, A.; Jonas, V.; Kohler, K. F.; Stegmann, R.; Veldkamp, A.; Frenking, G. *Chem. Phys. Lett.* **1993**, *208*, 111.
(33) Hollwarth, A.; Bohme, M.; Dapprich, S.; Ehlers, A. W.; Gobbi, A.; Jonas, V.; Kijhler, K. F.; Stegmann, R.; Veldkamp, A.; Frenking, G. *Chem. Phys. Lett.* **1993**, *208*, 237.
(34) Bergner, A.; Dolg, M.; Kuechle, W.; Stoll, H.; Preuss, H. *Mol. Phys.* **1993**, *80*, 1431.
(35) Dolg, M.; Wedig, U.; Stoll, H.; Preuss, H. *J. Chem. Phys.* **1987**, *86*, 866.
(36) Glendening, E. D.; Read, A. E.; Carpenter, J. E.; Weinhold, F. *NBO (version 3.1)*; Gaussian, Inc.: Pittsburgh, PA, 2003.
(37) The CCSD(T)/BS1//B3LYP/BS1 calculations also indicate that **1Fe** is only 0.4 kcal/mol more stable than **2Fe**. In conflict with the experiment that showed **1Fe** is the only species isolated, our results predict that both **1Fe** and **2Fe** should be isolated. At present, we have no explanation for this discrepancy.
(38) Ng, S. M.; Huang, X.; Wen, T. B.; Jia, G.; Lin, Z. *Organometallics* **2003**, *22*, 3898.
(39) Schleyer, P. v. R.; Maerker, C.; Dransfeld, A.; Jiao, H.; Hommes, N. J. R. v. E. *J. Am. Chem. Soc.* **1996**, *118*, 6317.
(40) All attempts to find a transition state for a 3,5-metal migration were unsuccessful and led to the formation of a transition state for η^5-Cp/η^1-Cp interconversion.
(41) Wright, M. E.; Nelson, G. O.; Glass, R. S. *Organometallics* **1985**, *4*, 245.
(42) Nyulászi, L.; Schleyer, P. v. R. *J. Am. Chem. Soc.* **1999**, *121*, 6872.
(43) Crabtree, R. H. *The Organometallic Chemistry of the Transition Metals*, 4th ed.; Wiley: New York, 2005, pp. 32.
(44) Rayón, V. M.; Frenking, G. *Organometallics* **2003**, *22*, 3304.
(45) Tanabe, M.; Bourke, S. C.; Herbert, D. E.; Lough, A. J.; Manners, I. *Angew. Chem., Int. Ed.* **2005**, *44*, 5886.
(46) Herbert, D. E.; Tanabe, M.; Bourke, S. C.; Lough, A. J.; Manners, I. *J. Am. Chem. Soc.* **2008**, *130*, 4166.

JP810032A